PHYSICAL REVIEW B **76**, 220501(R) (2007)

Phonons in superconducting CaC_6 studied via inelastic x-ray scattering

M. H. Upton,[1] A. C. Walters,[2,3] C. A. Howard,[2] K. C. Rahnejat,[2] M. Ellerby,[2] J. P. Hill,[1] D. F. McMorrow,[2,3] A. Alatas,[4] Bogdan M. Leu,[4] and Wei Ku[1]

[1]*Condensed Matter Physics and Materials Science Department, Brookhaven National Laboratory, Upton, New York 11973, USA*

[2]*London Centre for Nanotechnology and Department of Physics and Astronomy, University College London, London WC1E 6BT, United Kingdom*

[3]*ISIS Facility, Rutherford Appleton Laboratory, Chilton, Didcot, United Kingdom*

[4]*Advanced Photon Source, Argonne National Laboratory, Argonne, Illinois 60439, USA*

(Received 7 September 2007; published 4 December 2007)

We investigate the dispersion and temperature dependence of a number of phonons in the recently discovered superconductor CaC_6 utilizing inelastic x-ray scattering. Four [00*L*] and two *ab*-plane phonon modes are observed, and measured at temperatures both above and below T_c. In general, our measurements of phonon dispersions are in good agreement with existing theoretical calculations of the phonon dispersion. This is significant in light of several discrepancies between experimental measurements of phonon-derived quantities and theoretical calculations. The present work suggests that the origin of these discrepancies lies in the understanding of the electron-phonon coupling in this material, rather than in the phonons themselves.

DOI: 10.1103/PhysRevB.76.220501 PACS number(s): 74.25.Kc, 74.70.−b, 78.70.Ck

CaC_6 has attracted a great deal of interest since the recent discovery of its superconductivity below 11.4 K.[1,2] The transition temperature is atypical for graphite intercalation compounds, where transition temperatures are, with one exception, an order of magnitude lower. (The second highest known transition temperature, of YbC_6, is still nearly 50% lower, 6.5 K.) Despite an intriguing initial suggestion of an unconventional pairing mechanism[3] much of the early experimental evidence indicates that CaC_6 is a conventional weakly coupled superconductor.[4,5] Still, the unusually high transition temperature has prompted a great deal of speculation as to which phonons play a part in pairing and why the transition temperature is so high.[4–9]

Calandra and Mauri[6] and Kim *et al.*[4] have calculated the phonon spectra and the electron-phonon coupling using density functional theory (DFT). Both predict electron-phonon coupling with the Ca_c (out-of-plane) and C_{ab} (in-plane) modes. While these two calculations of the phonon dispersions are similar, their predictions of the coupling differ, with Calandra and Mauri assigning additional coupling to the C_{ab} modes.

There are a number of discrepancies between the theoretically calculated phonon spectra and electron-phonon coupling and a variety of phonon-derived experimental quantities for this system—as outlined in a recent paper by Mazin *et al.*[10] For example, recent measurements of the isotope effect, $\alpha(X)=-(d\log T_c/dM_X)$ (where T_c is the superconducting transition temperature and M_X is the mass of atom X) have found $\alpha(\mathrm{Ca})=0.53$,[11] in disagreement with the calculated value of $\alpha(\mathrm{Ca})=0.24$.[6] This suggests that the coupling to soft Ca modes is greater than predicted by calculation. Furthermore, the measured temperature dependence of the specific heat does not show the large coupling effects derived from the calculated electron-phonon spectral function, $\alpha^2F(\omega)$.[4,10] (Also called the Eliashberg function, $\alpha^2F(\omega)$ is a measure of the electron-phonon coupling. $F(\omega)$ is the phonon density of states.[12]) Thus, in contrast to the isotope effect measurements discussed above, specific heat experiments suggest that the coupling to acoustic Ca modes is significantly weaker than is predicted by theory.

Additionally, the upper critical field of CaC_6 has been shown to have a linear temperature dependence down to 1 K while calculations of the upper critical field, based on LDA calculations of $\alpha^2F(\omega)$, have predicted nonlinear behavior below 4 K.[7,10,13] Finally, DFT calculations of the phonon spectra understate the increase of T_c under pressure by an order of magnitude.[4,14,15]

The measurements of the isotope effect and the specific heat appear to lead to contradictory conclusions, since the isotope measurement implies larger-than-calculated coupling to soft Ca modes while the specific heat measurements suggest less-than-calculated coupling to soft Ca modes. This apparent conflict rests on a comparison of experimental results to theoretical predictions which yield $\lambda\sim 0.85$.[4,6] However, a recent measurement suggests that the superconducting gap is 2.3 meV, 40% larger than previously measured.[16] Such a large gap suggests that CaC_6 is a strongly coupled superconductor.

It is clear that the theoretical understanding of CaC_6 is by no means complete, and in particular a number of experimental observations of quantities that are either directly or indirectly related to the phonon spectra are inconsistent with the present theoretical description. Given this situation it is clearly of great interest to measure the phonon spectra and compare it to the existing theoretical predictions.[4,6]

In this paper we report measurements of the phonon dispersions in CaC_6, utilizing inelastic x-ray scattering (IXS) to do so. In particular, we have measured the dispersion, and temperature dependence of the dispersion, for a number of the low energy modes, including soft Ca_{ab} modes and part of the C_{ab} mode, that are believed to be important in the superconductivity of the CaC_6.[6,7] In general, we find good agreement with the extant predictions for the phonon dispersion curves. These results apparently confirm the validity of the DFT approach used in such calculations and suggest that the origin of the various discrepancies with experiment dis-

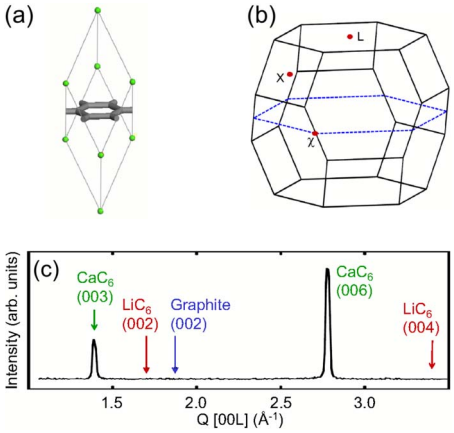

FIG. 1. (Color online) (a) CaC_6 crystal structure (Ref. 2). Green circles represent Ca atoms and the gray ring is graphene (Ref. 19). (b) The CaC_6 Brillouin zone. (c) An [00L] diffraction pattern taken after the inelastic experiment. The pattern exhibits sharp CaC_6 (003) and (006) peaks. The locations of possible impurity peaks from LiC_6 and graphite are indicated. Almost no scattering is observed at these locations.

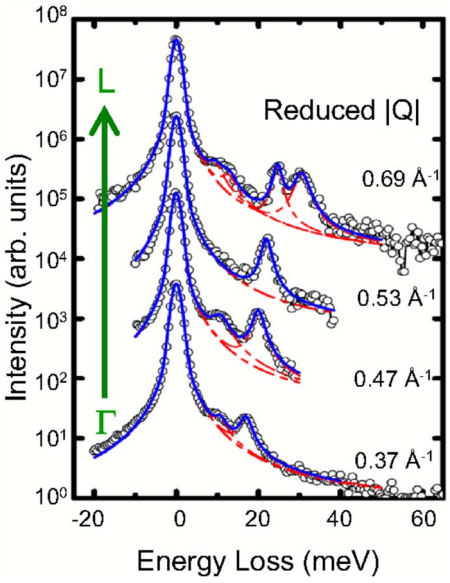

FIG. 2. (Color online) Inelastic spectra along Γ-L from the fourth Brillouin zone. As discussed in the text, the phonon cross section means that some of the phonon modes reported in Fig. 3 do not appear in these data. Data are labeled by momentum transfer in the reduced zone scheme. The spectra are offset for clarity and are normalized to account for the different efficiencies of the different detectors. The y axis is a $\log_{10}$ scale. The blue (dark gray) solid lines are the total fit. Each red (light gray) short-long dashed line is a portion of the total fit, including the elastic line and one phonon mode peak.

cussed above lie in the understanding of the electron-phonon coupling not of the phonon modes themselves.

The samples were prepared via immersion of a highly orientated pyrolytic graphite (HOPG) platelet in a lithium/calcium alloy for 10 days, as described in detail by Pruvost *et al.*[17] The HOPG was ZYA grade purchased from GE Advanced Ceramics with an initial (nonintercalated) highly-aligned c-axis mosaic of $\sim 0.4°$. It is powderlike in the ab-plane. The lithium and calcium were purchased from Sigma-Aldrich at 99.99% purity. X-ray diffraction of the resulting shiny silver CaC_6 platelet is shown in Fig. 1(c). Diffraction showed very high sample purity with the intensity of the (002) Bragg peaks of the LiC_6 phase and the graphite phase having less than 0.25% the intensity of the CaC_6 (006) Bragg peak.

The sample dimensions were $4 \times 4 \times 0.7$ mm with a postintercalation c-axis mosaic of $\sim 3.5°$. The crystal structure and Brillouin zone of CaC_6 (space group $R\bar{3}m$, $a=5.17$ Å, $\alpha=49.55$) are shown in Figs. 1(a) and 1(b).[2]

After synthesis, the samples were mounted in a beryllium dome in an argon or helium atmosphere. The region around the beryllium dome was subsequently pumped out to rough vacuum. The diffraction pattern of the sample was checked before, after, and several times during the experiment. Both the out-of-plane diffraction patterns and the rocking curves of the (003) and (006) reflections were monitored during the experiments and did not show any signs of degradation.[18] A postexperiment diffraction pattern is shown in Fig. 1(c).

The IXS experiments were performed at sector 3 at the Advanced Photon Source of Argonne National Laboratory.[20,21] Data were collected using Si(18 6 3) analyzer reflections. The instrument had an overall resolution of 2.3 to 2.5 meV. Photon flux was $(1.8-2.4) \times 10^9$ photons/s. Four analyzer crystals and four independent detectors allowed data collection at four momentum transfers simultaneously. The momentum resolution was 0.072 $Å^{-1}$ in the scattering plane and 0.18 $Å^{-1}$ perpendicular to it. The beam size at the sample was 250×300 μm. The spectra were normalized by a beam intensity monitor immediately before the sample. Spectra with $\vec{Q}$ in the [00L] direction were measured in reflection geometry while spectra with $\vec{Q}$ in the ab-plane were measured in transmission geometry. Finally, we note that identical results were obtained from two samples, prepared at different times and measured in separate runs.

A series of spectra taken at 5 K with $\vec{Q}$ in the [00L] direction and in the fourth Brillouin zone, with $\vec{Q}$ between $\frac{3}{2}\vec{G}$ and $2\vec{G}$ where $\vec{G}$ is one reciprocal lattice vector, are shown in Fig. 2. Typical phonon intensities are <1 count/s. Example fits are shown in the figure. The elastic line is fit with a psuedovoigt while the phonon peaks are fit with Lorentzians. Near the L point zone boundary, the feature at 10 meV is seen to broaden, and a better fit is obtained if the data are fit to two modes.

A summary plot showing the resulting peak positions is shown in Fig. 3. Note that not all of the phonon observations reported in Fig. 3 are visible in Fig. 2 because the cross section of different phonons varies with momentum transfer. Specifically, the phonon intensity is proportional to $(\vec{Q} \cdot \vec{\epsilon})^2/\hbar\omega$, where $\vec{\epsilon}$ is the atomic displacement, $\vec{Q}$ is the momentum transfer, and $\hbar\omega$ is the energy of the phonon mode. Some phonons shown in Fig. 3 are visible only in higher Brillouin zones or at longer counting times. The data in Fig. 3(a) are shown in a reduced zone scheme with spectra

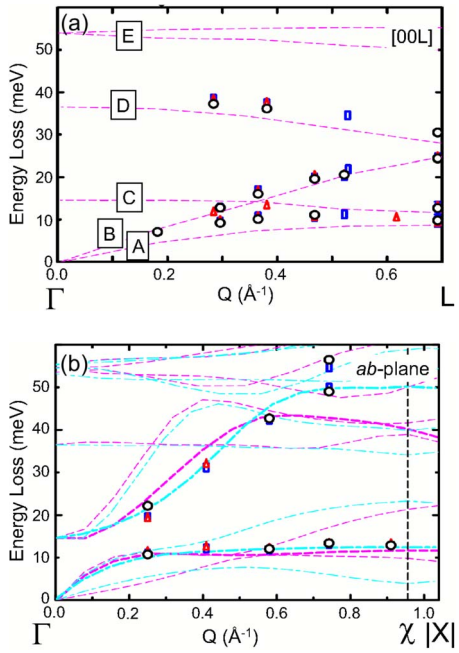

FIG. 3. (Color online) Phonon dispersion from spectra taken at three different temperatures: 300 K in circles, ○; 50 K in triangles, △; and 5 K shown in squares, □. (a) The $[00L]$ spectra. Calculated dispersions are shown as dashed lines (Ref. 6) Different calculated modes are labeled by $A-E$. (b) The *ab*-plane spectra. The distance to χ is indicated by a vertical black long dashed line. The Γ-X calculated dispersions are shown as pink long dashed lines and the Γ-χ dispersions are shown as blue short-long dashed lines. Note that Γ-X is not a strictly *ab*-plane dispersion. The theoretical curves most closely corresponding to the data shown are marked with thicker lines than other curves.

from different Brillouin zones folded back into the first Brillouin zone.

We discuss first the Γ-L dispersion [Fig. 3(a)]. Four phonon bands are observed in this direction. The lowest energy band, labeled A, is almost dispersionless over the measured region and has an energy near 10 meV. The second band, labeled B, disperses from 0 meV to 25 meV. A small portion of a third band, labeled C, can be seen near L near 10 meV. The final observed band, labeled D, disperses between 25 and 40 meV.

It is difficult to assign an exact cross section to a particular mode because the data were collected in different geometries. The elastic intensity is a reasonable, but imperfect, measure of the amount of material in the scattering volume, and additional factors complicate the comparison of data taken in the reflection $[00L]$ and transmission (*ab*-plane) geometries. However, we can report the relative cross sections of various modes at a particular momentum transfer in the $[00L]$ direction. At $\vec{Q}=2.08$ Å^{-1}, which corresponds to a reduced $\vec{Q}=0.69$ Å^{-1}, modes C and D have roughly equal intensities of 0.5 counts/s while mode A has an intensity of roughly 0.1 counts/s at 5 K. These count rates represent the raw data and are not scaled by the IXS polarization factor, $(\vec{Q}\cdot\vec{\epsilon})^2/\hbar\omega$.

Also shown in Fig. 3(a) are calculations of the phonon bands.[6] The two calculations agree to within a few meV in the measured energy range with the exception of the dispersion of the lowest energy optical band in the *ab*-plane.[4,6] The calculation of Calandra and Mauri[6] agrees with the data somewhat better than the calculation of Kim *et al.*,[4] so it is shown here. Moreover, Calandra and Mauri identify the phonon mode associated with each calculated band[6]. By comparison of our experimental data with this calculation, we identify mode A as a primarily Ca_{ab} oscillation with some C_c character, mode B as a mixed Ca_c and C_c mode, and mode D as a mixed Ca_c and C_c mode.[6]

In general the agreement between theory and experiment is good, though we note that the calculations of modes A and D understate the energy of the measured band throughout the dispersion. In addition, there are predicted modes that are largely or entirely absent in our data: Modes C and E. This apparent absence does not necessarily mean that the mode does not occur. In particular, mode C is predicted to have primarily Ca_{ab} character, which, because of the phonon polarization factor in the IXS cross section, means it should not be observed. This mode also has a small amount of C_c character, in addition to the majority Ca_{ab} component. A small C_c amplitude may be why these measurements observe the C mode in only a small portion of reciprocal space. In fact, mode A is also predicted to have primarily Ca_{ab} character and a small amount of C_c character, consistent with this. Near $\vec{Q}=1.24$ Å^{-1} the measured intensity of this mode is 45 times larger in the *ab*-plane than it is in the $[00L]$ direction (after scaling by the elastic intensity). Thus the polarization factor also explains the asymmetry in the intensity of this mode.

Despite measuring a wide range around 50 meV we are not able to observe 50 meV C_c phonons modes. Spectra were counted for between 80 and 120 seconds per 0.25 meV step. We believe that a 10 count peak would have been observable, which places an upper bound on any such mode of 0.1 counts/s at 300 K, less than 10% of the dispersing phonon band at similar momentum transfers. A related C_c phonon mode was also not observed in an IXS measurement on graphite.[22] We speculate that the amplitude of these modes is very small or the lifetime is very short (resulting in a broad peak). Either of these effects, when combined with the high predicted energy of mode E, would result in a very small IXS intensity.

Next we turn to the *ab*-plane phonons [Fig. 3(b)]. The interpretation of the *ab*-plane phonons is somewhat complicated because the data are not taken at a point in reciprocal space. Rather, because the sample is not oriented in-plane, each spectra is taken at fixed $|\vec{Q}|$, which represents an average over a circle in the *ab*-plane in reciprocal space of radius $|\vec{Q}|$, centered at Γ. Therefore, phonons which have a significant anisotropic dispersion in the *ab*-plane are not visible in these experiments because this anisotropy will translate into an energy broadening of the measured mode and consequently a reduction in the peak intensity. Of course, if the *ab*-plane dispersion is isotropic (identical in all *ab*-plane directions) the average is irrelevant and the mode may be observed. Finally, all the data must be taken in the first Brillouin zone because the powder structure of the *ab*-plane and

the unequal distances of different *ab*-plane directions in the Brillouin zone mean that phonon positions cannot be folded back to the first Brillouin zone. Despite these difficulties two phonon bands are observed. The flat band near 10 meV and a highly dispersive band which we measure between 15 and 50 meV. At $\vec{Q}=0.58$ Å^{-1} and 5 K, the two measured *ab*-plane phonon modes have roughly equal intensities of 0.1 counts/s.

Comparison with Calandra and Mauri (Fig. 3) identifies the low energy band as a principally Ca_{ab} mode and the dispersing band as a C_{ab} mode.[6] This latter mode, which is the *ab*-plane extension of mode *C* measured in the $[00L]$ direction, discussed above, disperses to higher energy than predicted.[4] A second highly dispersing C_{ab} mode is predicted by Calandra and Mauri, but is not observed.[6] This may be because the band is not isotropic. In fact, the principal difference (below 60 meV) of the calculations of Calandra and Mauri and Kim *et al.* is that Calandra and Mauri predict two isotropic C_{ab} bands dispersing from Γ at 15 meV while Kim *et al.* predict that only one of them is isotropic.

Calandra and Mauri[6] and Kim *et al.*[4] both predict a flat, isotropic band near 38 meV. This mode is not observed in experiments, which cannot be due to the *ab*-plane averaging effects discussed above. Thus its absence in the experimental data is explained by its assignment as a mixed Ca_c and C_c mode: The IXS polarization factor would suppress any such mode in this geometry.

Finally, the phonon dispersion is measured at three temperatures: 5 K, which is below the 11.4 K transition temperature, 50, and 300 K. No differences in the phonon spectra at different temperatures are observed, within the limits of our measurements. Additionally, there are no significant changes in the widths. Also, the intensity of the peaks appears to follow the temperature dependence predicted by Bose statistics, as expected.

In summary, we find good agreement between experiment and theory, although calculation underestimates the energy of two modes in the $[00L]$ direction. This agreement has a number of implications for the general understanding of the system. One immediate consequence is that the predicted $F(\omega)$, the phonon density of states, appears to be largely correct.[4,6]

Nevertheless, as discussed in the introduction, serious disagreements exist between experiment and the theoretical understanding of the system. The slight disparity between the calculated and measured $F(\omega)$ is probably not sufficient to reconcile these results. The disagreements are largely a result of predictions made using the calculated $\alpha^2F(\omega)$.[4,6] Thus, by confirming our understanding of the phonon dispersion, and hence the calculated $F(\omega)$, the present work raises serious questions about the calculation of the electron-phonon coupling. We hope that this work inspires theoretical studies to reconcile the existing discrepancies with experimental data.

We acknowledge helpful discussions with T. Berlijn. Work performed at BNL was supported by US DOE, Division of Materials Science and Engineering, under Contract No. DE-AC02-98CH10886 and partially by DOE-CMSN. Use of the Advanced Photon Source was supported by the US DOE, Office of Science, Basic Energy Sciences, under Contract No. DE-AC0Z-06CH11357. Work performed at UCL was supported by the UK Engineering and Physical Science Research Council and by the Wolfson Royal Society.

[1] T. E. Weller, M. Ellerby, S. S. Saxena, R. P. Smith, and N. T. Skipper, Nat. Phys. **1**, 39 (2005).
[2] N. Emery, C. Hérold, M. d'Astuto, V. Garcia, C. Bellin, J. F. Marêché, P. Lagrange, and G. Loupias, Phys. Rev. Lett. **95**, 087003 (2005).
[3] G. Csányi, P. B. Littlewood, A. H. Nevidomskyy, C. J. Pickard, and B. D. Simons, Nat. Phys. **1**, 42 (2005).
[4] J. S. Kim, L. Boeri, R. K. Kremer, and F. S. Razavi, Phys. Rev. B **74**, 214513 (2006).
[5] G. Lamura, M. Aurino, G. Cifariello, E. Di Gennaro, A. Andreone, N. Emery, C. Hérold, J.-F. Marêché, and P. Lagrange, Phys. Rev. Lett. **96**, 107008 (2006).
[6] M. Calandra and F. Mauri, Phys. Rev. Lett. **95**, 237002 (2005).
[7] J. S. Kim, R. K. Kremer, L. Boeri, and F. S. Razavi, Phys. Rev. Lett. **96**, 217002 (2006).
[8] I. I. Mazin, Phys. Rev. Lett. **95**, 227001 (2005).
[9] L. Boeri, G. B. Bachelet, M. Giantomassi, and O. K. Andersen, Phys. Rev. B **76**, 064510 (2007).
[10] I. I. Mazin, L. Boeri, O. V. Dolgov, A. A. Golubov, G. B. Bachelet, M. Giantomassi, and O. K. Andersen, Physica C **460**, 116 (2007).
[11] D. G. Hinks, D. Rosenmann, H. Claus, M. S. Bailey, and J. D. Jorgensen, Phys. Rev. B **75**, 014509 (2007).
[12] J. P. Carbotte, Rev. Mod. Phys. **62**, 1027 (1990).
[13] E. Jobiliong, H. D. Zhou, J. A. Janik, Y.-J. Jo, L. Balicas, J. S. Brooks, and C. R. Wiebe, Phys. Rev. B **76**, 052511 (2007).
[14] M. Calandra and F. Mauri, Phys. Rev. B **74**, 094507 (2006).
[15] A. Gauzzi, S. Takashima, N. Takeshita, C. Terakura, H. Takagi, N. Emery, C. Hérold, P. Lagrange, and G. Loupias, Phys. Rev. Lett. **98**, 067002 (2007).
[16] C. Kurter, L. Ozyuzer, D. Mazur, J. F. Zasadzinski, D. Rosenmann, H. Claus, D. G. Hinks, and K. E. Gray, Phys. Rev. B **76**, 220502 (2007).
[17] S. Pruvost, C. Hérold, A. Hérold, and P. Lagrange, Carbon **42**, 1825 (2004).
[18] One of the first diffraction signs of degradation in air exposure is the increase in width of the (006) rocking curve relative to the (003) rocking curve.
[19] This figure was generated using a software program from Accelrys.
[20] H. Sinn, Nucl. Instrum. Methods Phys. Res. A **467-468**, 1545 (2001).
[21] H. Sinn, J. Phys.: Condens. Matter **13**, 7525 (2001).
[22] M. Mohr, J. Maultzsch, E. Dobardžić, S. Reich, I. Milošević, M. Damnjanović, A. Bosak, M. Krisch, and C. Thomsen, Phys. Rev. B **76**, 035439 (2007).